PAPER

Fructose controlled ionophoric activity of a cholate–boronic acid†

James R. D. Brown, Inmaculada C. Pintre and Simon J. Webb*

Wulff-type boronic acids have been shown to act as ionophores at pH 8.2 by transporting Na^+ through phospholipid bilayers. A cholate–boronic acid conjugate was synthesised and shown to be an ionophore, although the hydroxyl-lined face of the cholate moiety did not enhance ion transport. Mechanistic studies suggested a carrier mechanism for Na^+ transport. The addition of fructose (>5 mM) strongly inhibited ionophoric activity of the cholate–boronic acid conjugate, mirrored by a strong decrease in the ability of this compound to partition into an organic phase. Modelling of the partitioning and ion transport data, using a fructose/boronic acid binding constant measured at pH 8.2, showed a good correlation with the extent of fructose/boronic acid complexation and suggested high polarity fructose/boronic acid complexes are poor ionophores. The sensitivity of ion transport to fructose implies that boronic acid-based antibiotic ionophores with activity modulated by polysaccharides in the surrounding environment may be accessible.
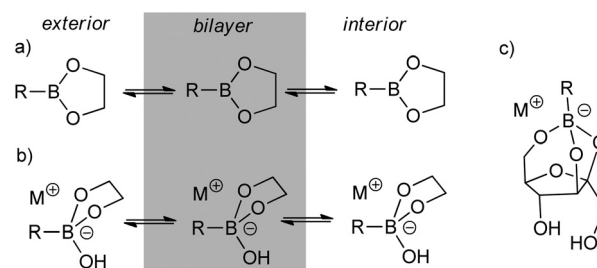
Introduction

The recognition of polyols, in particular saccharides, by boronic acids is an example of a dynamic covalent chemistry that has provided a wealth of applications in supramolecular chemistry, with recent examples in sensing,[1] drug delivery,[2] separation[3] and hydrogel formation.[4] The interaction of lipophilic or membrane-bound boronic acids with saccharides or glycolipids has risen to particular prominence in recent years,[5,2b] driven in part by the development of 2-(hydroxymethyl)phenylboronic acids able to bind a wider range of sugars at close to physiological conditions.[6] Lipophilic boronic acids have also been known for some time to also transport saccharides, particularly fructose, across supported membranes,[7] bulk organic phases[8] and phospholipid bilayers.[9]

Amphiphilic boronic acids are suggested to transport saccharides by forming complexes that are sufficiently lipophilic to diffuse across the membrane. Two mechanisms have been proposed for boronic acid-mediated diol transport across membranes (Fig. 1), with transport either occurring through trigonal planar boronate esters or tetrahedral boronate anions; the pH of the sending phase and boronic acid pK_a determines which mechanism is followed.[10] A cation is associated with

Fig. 1 Scheme showing the transport of boronic acid–diol complexes through bilayers either as (a) trigonal planar or (b) tetrahedral boron species. (c) Main 1 : 1 boronate complex formed with fructose.[12]

tetrahedral boronate anions, which can be covalently linked to the boronic acid, an added lipophilic tetraalkylammonium salt, or it can be a counterion symported with the sugar from the sending phase.[7,11] In the latter case a crown ether is often added to form a lipophilic complex able to pass through the apolar membrane phase.[10a] Despite the implication that cation transport is concomitant with saccharide transport transport,[7,9b,11] boronic acid mediated M^+ transport across phospholipid bilayers has not been explicitly measured and compared to the rate of concomitant saccharide transport.

The ability of lipophilic boronic acids embedded in phospholipid bilayers to complex sugars suggests new ways of controlling ion flux across phospholipid bilayers, with ion flow across the membrane controlled by the presence of biological catechols[13] or saccharides.[14] Saccharides are ideal for controlling ion transport as these highly polar molecules cannot cross the phospholipid bilayer, they will not discharge a pH gradient

Manchester Institute of Biotechnology (MIB) and School of Chemistry, University of Manchester, 131 Princess St., Manchester M1 7DN, UK.
E-mail: S.Webb@manchester.ac.uk
†Electronic supplementary information (ESI) available: NMR spectra of **3**. K^+ transport by **3**. U-tube picrate transport data. Effect of fructose on Na^+ transport by **3** or **4**. See DOI: 10.1039/c4ob00165f

2576 | *Org. Biomol. Chem.*, 2014, **12**, 2576–2583

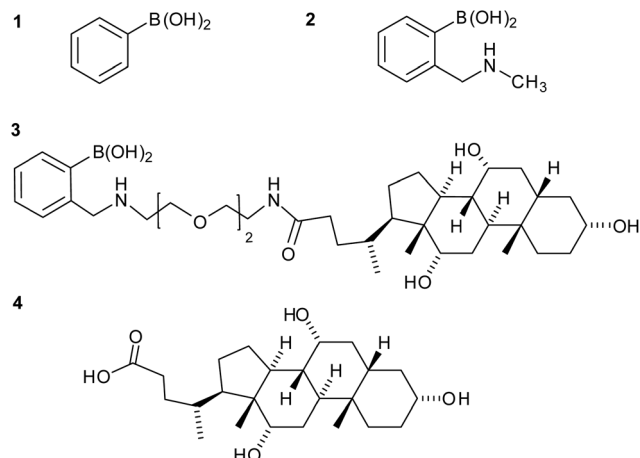This journal is © The Royal Society of Chemistry 2014

Fig. 2   Boronic acids and cholic acid.

and unlike lipophilic polyols they will not disrupt bilayer membranes. Although the affinities of sugars for most boronic acids is generally rather weak, some sugars, such as fructose, exhibit binding constants with phenylboronic acids in buffer in the order of 100 M^{-1}.

Previously we developed cholate-based ionophores that can be turned on or off by complexation to metal ions or proteins.[15] Adding boronic acid mediated recognition/transport with mono- or bis-cholate scaffolds was expected to provide some interesting ionophores, especially as oligocholates are known to transport metal ions and dyes through bilayers, through either channel or carrier mechanisms.[16,17] The high activity of cholates stems from their facial amphiphilicity, which provides hydrophobic convex surfaces that can be presented to the bilayer and concave hydrophilic surfaces that can interact with alkali metal ions.

Linking cholates with boronic acids was hoped to produce saccharide-switchable ion transport across phospholipid bilayers. Fructose forms boronic acid complexes with a variety of geometries and stoichiometries,[12] including 1 : 2 fructose to boronic acid,[12,18] and we wondered if fructose could assemble boronic acid–cholate conjugates into dimers that might form channels[17] or "hairpin" carriers with a sequestered hydrophilic cavity. The compounds we investigated for cation transport ranged from phenylboronic acid **1** and Wulff-type 2-(N-methyl-aminomethyl)phenylboronic acid **2**, to a more amphiphilic Wulff-type boronic acid conjugate **3** that has a single facially amphiphilic cholate tail (Fig. 2).

Results and discussion

Synthesis of 3

Boronate-cholate derivative **3** was synthesised in two steps from cholic acid **4**. The short triethylene glycol spacer was added between the cholate body and the boronic acid to give flexibility around the complexation site and to project it away from the cholate, which will become embedded in the bilayer.

Cholic acid **4** was first coupled to mono-protected 1-(benzyl-oxycarbonylamino)-3,6-dioxa-8-aminooctane, the product hydrogenolysed, then reductively aminated with 2-formyl-phenylboronic acid to give compound **3** in 59% yield from the acid.

Ion transport assays

To screen the ability of these compounds to transport cations through bilayers we chose the phospholipid vesicle based 8-hydroxypyrenetrisulfonate (HPTS pK_a = 7.3) assay,[19] using an interior pH of 6.5 and an exterior pH of 8.5. The exterior pH was selected to be above the pK_a of aminomethylboronic acids ($pK_a \sim 6.5$)[7] and corresponding saccharide complexes ($pK_a <$ 6.5),[20] a strategy designed to favour M^+/OH^- co-transport. EYPC/cholesterol vesicles were used as these bilayers have the right balance between fluidity and impermeability. Fluidity allows assembly in the membrane and diffusion through the membrane, but pure EYPC bilayers gave unsatisfactory levels of background leakage.

The choice of buffer was crucial as boronic acid complexation of diols is strongly pH dependent, with the ideal pH between the pK_a of the diol and the boronic acid.[21] Buffer type and concentration can also strongly affect the binding of boronic acids to saccharides, with stronger binding at low buffer concentrations.[22] To obtain precise pH control, the standard procedure for the HPTS assay was modified, with HPTS-loaded vesicles directly added to buffer at pH 8.5 rather than addition of an external aliquot of NaOH (the base pulse). The ionophore was then added after 180 s to initiate transport, which also eliminates the jump in fluorescence observed if the base pulse is applied after ionophore addition.

Initially cholate–boronic acid **3** was assayed for its ability to allow sodium ions to cross a bilayer. Addition of cholate–boronic acid **3** (10 μM) to give a membrane loading of 5% mol/mol gave an immediate increase in fluorescence that suggested Na^+/H^+ antiport or Na^+/OH^- symport across the bilayer of these EYPC/chol vesicles. Cholic acid **4** ($pK_a \sim 4.6$)[23] did not conduct sodium ions across the membrane and gave little transport above the background methanol control (Fig. 3).

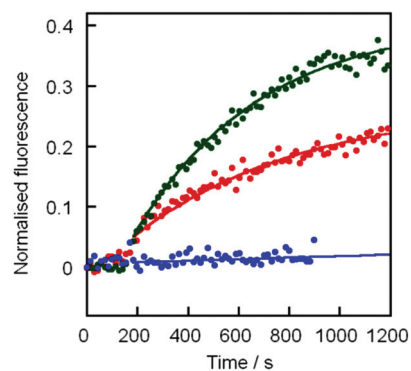**Fig. 3**   Transport of Na^+ across EYPC/chol bilayers by boronic acid **2** (●), boronate-cholate **3** (●) and cholate **4** (●). The methanol control has been subtracted from the data. First order curve fits are to guide the eye.

This journal is © The Royal Society of Chemistry 2014

Org. Biomol. Chem., 2014, **12**, 2576–2583 | **2577**

To confirm that the boronic acid is the active moiety in mediating ion transport, phenylboronic acid **1** and 2-(*N*-methylaminomethyl)phenylboronic acid **2** were also assessed for their ability to transport Na⁺ through an EYPC/chol bilayer. Phenylboronic acid (10 μM, 5% mol/mol) did not transport sodium ions above the background rate, but the 2-(*N*-methyl-aminomethyl) derivative **2** (10 μM, 5% mol/mol) gave good transport of Na⁺ at a rate above that observed for cholate boronic acid **3**. This observation suggests that the cholate hydroxyls play little role in assisting ion transport and the sodium ion is co-transported in close proximity to an anionic boronate headgroup. The pK_a of **2** is ~6.5,[7] and at pH 8.5 the major species in solution will be the tetrahedral boronate anion, but phenylboronic acid **1** has a higher pK_a of 8.8,[21a,22] suggesting that at pH 8.5 the major boron species in solution will be uncharged; this trigonal planar boronic acid would be unable to antiport Na⁺/H⁺ or symport Na⁺/OH⁻ across the membrane.

Effect of fructose on ion transport

Based upon literature binding constants (K from 100 to 500 M⁻¹) in methanol–buffer mixtures at near neutral pHs,[22,24,25] we hoped that 100 mM fructose would be sufficient to give extensive complexation of the boronic acid headgroups in these ionophores. The effect of this concentration of fructose on ion transport by ionophore **3** was assessed using the HPTS assay. During formation and purification of the EYPC/chol vesicles, all pH 6.5 buffer solutions also contained 100 mM fructose, maintaining the osmotic balance across the vesicle membrane. As previously, an aliquot of this vesicle solution was transferred to iso-osmotic buffer with 100 mM fructose at pH 8.5 before ionophore **3** was added at 180 s. Under these conditions, little Na⁺ transport was observed, with discharge of the pH gradient only marginally above the methanol control (Fig. 4a). As expected the low level of transport exhibited by cholate control **4** was found to be little affected by the addition of fructose (ESI Fig. S3†). A similar switching off of ion transport was observed for boronate **2** in the presence of 100 mM fructose, showing that complexation to fructose diminished

the ability of these Wulff-type boronic acids to act as ionophores.

If the complexation of the boronic acid group to fructose blocks the activity of these ionophores, then the rate of Na⁺ transport should depend on the fructose concentration. Ion transport by **3** was monitored in the presence of 2.5 mM, 5 mM, 10 mM and 100 mM fructose, which revealed a steady decrease in activity as the concentration of fructose increased. A plot of the extent of transport after 1200 seconds against the concentration of fructose showed an inverse dependence, a relationship that mirrors the fraction of free ionophore **3** expected at different concentrations of fructose (Fig. 4b).

Mechanistic investigations

Smith and co-workers have shown that boronic acids transport saccharides across bilayers *via* a carrier mechanism, which implies a similar mechanism for Na⁺ transport by **2** and **3**. A classical test for an ion carrier mechanism is the ability to transport ions through a bulk organic phase in a U-tube experiment.[19] The boronic acids **2** and **3** were assessed for their ability to transport sodium picrate across a chloroform phase, using 0.01% wt/vol sodium picrate in sodium phosphate buffer (2.5 mL, 20 mM phosphate, 100 mM NaCl, pH 8.5) in the sending phase and sodium phosphate buffer (2.5 mL, 20 mM phosphate, 100 mM NaCl, pH 6.5) in the receiving phase. In addition, cholic acid **4** and dibenzo-18-crown-6 were also assessed for their ability to transport sodium picrate. Boronic acid **3** (1 mM) transported sodium picrate through the chloroform layer at a rate comparable to dibenzo-18-crown-6 (respectively 1% and 3% picrate transport after 6 h, ESI Fig. S5†).[26] As expected, cholate **4**, lacking the boronic acid, was unable to transport sodium picrate through the organic phase (~0.07% after 6 h). Surprisingly, boronic acid **2** was also relatively ineffective (0.2% after 6 h), which was ascribed to its fairly high solubility in the aqueous phase.

Given that lipophilic boronate complexes are known to transport fructose through organic phases,[7–9] the relationship between fructose transport and Na⁺ transport was also assessed. The ability of ionophore **3** to transport fructose/Na⁺ through the organic CHCl₃ phase was assessed using a U-tube and a combination of ¹H-NMR analysis (fructose transport) with UV-visible spectroscopy (Na⁺ transport). A CDCl₃ (99.8 atom % D) solution of **3** (1 mM) was transferred to a glass U-tube. A receiving phase of sodium phosphate buffer (D₂O containing 0.75% sodium 3-(trimethylsilyl)-2,2,3,3-d₄-propionate salt as an internal standard, 20 mM phosphate, 100 mM NaCl, pH 6.5) was added to one side of the U-tube, and to the other side was added a source phase of fructose (1 M) and 0.01% wt/vol sodium picrate in sodium phosphate buffer (D₂O containing 0.75% internal standard, 20 mM phosphate, 100 mM NaCl, pH 8.5). Aliquots were taken at intervals from the receiving phase and analysed by ¹H NMR spectroscopy for the presence of fructose, but no fructose transport was detected over 10 h. Similarly, UV-visible measurements of the receiving phase showed a concomitant lack of picrate in the receiving phase, confirming that little Na⁺ transport was
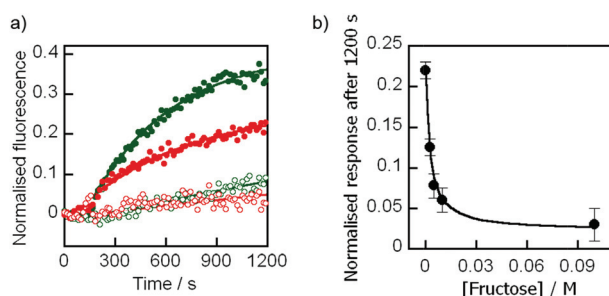

Fig. 4 (a) Transport of Na⁺ across EYPC/chol bilayers by **2** (●), **2** with 100 mM fructose (○), **3** (●) and **3** with 100 mM fructose (○). First order curve fits are to guide the eye. (b) Plot of Na⁺ transport by **3** after 1200 s at different concentrations of fructose. Curve fitted using eqn (2) with K = 400 M⁻¹.

2578 | *Org. Biomol. Chem.*, 2014, **12**, 2576–2583

This journal is © The Royal Society of Chemistry 2014

occurring. Both observations suggest that the fructose complex of **3** is too polar to efficiently partition into the apolar phase. The lack of fructose transport by **3** is similar to that observed by Karpa *et al.* for a cholesterol–phenylboronic acid conjugate, which they ascribed to slow diffusion across the aqueous–organic interface for very lipophilic boronic acids.[27]

To measure changes in lipophilicity caused by complexation to fructose, the distribution constant (K_D) for cholate boronic acid **3** and cholate **4** in the presence of fructose was measured. Solutions of **3** or **4** in 1-octanol (10 mM) were prepared and an equal volume of pH 8.5 buffer was added. The aqueous–organic mixture was vigorously mixed for 180 s before standing for 1 h. To calculate the concentration of **3** or **4** in the organic layer, the UV-visible absorbances (260 nm) of aliquots from the organic layer were measured. The same procedure was repeated for 0.01, 0.1 and 0.5 M fructose in pH 8.5 phosphate buffer. A plot of the buffer/octanol distribution constant (K_D) at pH 8.5 for ionophore **3** and cholic acid **4** as a function of changing fructose concentration revealed a strong decrease in the lipophilicity of **3** in the presence of fructose, decreasing from 2.0 in the absence of fructose to 1.2 at concentrations of fructose above 0.1 M. In contrast the pH 8.5 buffer/octanol distribution constant for cholic acid **4** was relatively unaffected by the presence of fructose, and was between 2.2 and 2.6 at all concentrations of fructose tested (Fig. 5a). These observations are consistent with ionophore **3** binding to fructose to produce a complex that is less able to partition into the membrane and mediate transport.

To allow us to model these changes in K_D, the binding affinity (K) of compound **2** for fructose was determined under conditions similar to those used for the HPTS assays (pH 8.5). By using pyrocatechol violet in a competitive displacement assay[28] and following the method developed by Wang,[22] the affinity of **2** for fructose in phosphate buffer (20 mM Na$_n$H$_m$PO$_4$, 100 mM NaCl, pH 8.5) was determined as $K \sim 230$ M^{-1}. The partition data for fructose + **3** were then fitted to a simple model, where the measured value of the distribution constant K_D(obs) will be an average of K_D and K'_D weighted according to the fraction of free boronate and fructose-boronate complex respectively (Fig. 5b). With the concentration of fructose much greater than the concentration of boronate, this gives the relationship below:

$$K_D(\text{obs}) = \frac{K_D + K'_D K[\text{fructose}]}{1 + K[\text{fructose}]} \qquad (1)$$

By approximating the values of K_D and K'_D from the distribution coefficients of **3** with and without 1 M fructose, combined with the approximate binding constant for **2** to fructose in pH 8.5 buffer, a good fit was found to the distribution constant data using eqn (1) (Fig. 5a).

This analogy was extended by fitting the HPTS responses for **3** after 1200 s (ESI Fig. S4†) to eqn (2). In this relationship, 1 is the normalised response in the absence of fructose, and 0.17 is the estimated normalised response at saturating fructose concentrations.
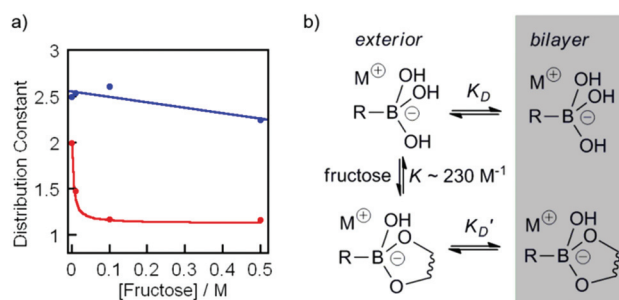
$$\text{Response} = \frac{1 + 0.17K[\text{fructose}]}{1 + K[\text{fructose}]} \qquad (2)$$

This equation gave a reasonable fit (Fig. 4b) with values of K between 300 and 400 M^{-1}, similar to the measured affinity of **2** for fructose and consistent with complexation of fructose inhibiting of ion transport. This agreement is remarkable given that ion transport recorded by an HPTS assay is a combination of factors, including the rate of ionophore distribution across the population of vesicles.[29a]

The similarity between the decline in ionophoric activity of **3** with increasing fructose and the decrease in K_D with increasing fructose suggests that ionophoric activity is modulated by the ability of the boronate to partition into the bilayer. Support for this suggestion comes from models of carrier-mediated ion transport across bulk organic phases.[30] By assuming that transport across a bilayer will be broadly analogous to transport through a bulk organic phase and that low saturation conditions exist at both bilayer–aqueous interfaces, diffusion of the Na$^+$/boronate complex through the buffer–bilayer interface would be the rate limiting step. The rate of transport across the bilayer would then be proportional to the ability of the ionophore to partition into the membrane.

Conclusions

2-(Methylaminomethyl)phenylboronic acids have been shown to transport Na$^+$ across phospholipid bilayers. Boronic acid–cholate conjugate **3** transported Na$^+$ through carrier rather than channel mechanisms despite cholate derivatives being well known to form channels in phospholipid bilayers.[16,17] The conjugate **3** was less effective than the smaller 2-(methylaminomethyl)phenylboronic acid **2** at transporting Na$^+$ across bilayers, perhaps due to slower diffusion through the membrane or slower redistribution across the vesicle population,[29] but **3** was more effective at transporting across a bulk organic phase. We have also shown that Na$^+$ transport by 2-(methylaminomethyl)phenylboronic acids **2** and **3** is not coupled to saccharide transport, and that fructose complexation instead switches off ion flow. Mechanistic studies suggest that

Fig. 5   (a) Changes in the distribution constant K_D for ionophore **3** (red, ●), and cholate **4** (blue, ●) in the presence of 0 M, 0.01 M, 0.1 M, and 0.5 M fructose. Curve fit added for **3** using eqn (1) and $K = 230$ M^{-1}, with linear curve fit for **4** to guide the eye. (b) Model mechanism for the partition of **3** into the bilayer in the presence of fructose.

complexation to fructose shuts down ionophoric activity due to the lower lipophilicity of the Na^+/saccharide/boronate complexes inhibiting partitioning into the bilayer.

The studies presented here may open a pathway towards saccharide-sensitive ionophores, provided that high selectivity for targeted saccharides under physiological conditions[6] can be engineered into the boronic acid moiety. Several design rules can be elucidated for the construction of such saccharide sensitive boronic acid ionophores. The boronic acid must be designed so that the pK_a lies below the pH of the sending (exterior) solution. It may not be necessary to have a crown ether or other Na^+ complexing site appended to the boronic acid for sodium ion transport,[11] as the hydroxyl-lined cholate on **3** did not provide greater activity than simple boronic acid **2**. Other simple saccharides should produce a different effect on ionophoric activity, depending upon binding constant and complex lipophilicity. Covalently linking together cholates into bis(cholate) dimers[17] with boronic acids at both termini did not give any improvement in Na^+ transport activity, and these compounds also followed a carrier mechanism with similar activity.[31] Transport of other cation/anion combinations are yet to be investigated, although preliminary studies indicate K^+ is transported in much the same way as Na^+ (ESI Fig. S6†).

Given recently reported biological applications of a new generation of boronates able to complex to polysaccharides under physiological conditions,[2b,5e,32] work is ongoing to generate new types of boronic acid-based antibiotics that are responsive to the concentration of targeted polysaccharides in the surrounding environment.

Experimental section

Benzeneboronic acid **1** and cholic acid **4** were purchased from Sigma-Aldrich and used as received. Phospholipids were obtained from Avanti Polar Lipids. Unless otherwise stated, all other reagents and solvents were obtained from commercial suppliers (Sigma-Aldrich, Fluka, Acros and Alfa Aesar). Anhydrous dichloromethane was obtained by distillation from calcium hydride, and anhydrous tetrahydrofuran was obtained by distillation from sodium. Thin layer chromatography (TLC) was carried out using Merck aluminum-backed F254 silica gel plates and visualised with either UV light (256 nm or 365 nm), alkaline aqueous $KMnO_4$, ninhydrin, 2,4-dinitrophenylhydrazine, or cerium molybdate. Preparative column (flash) chromatography was carried out using commercially available normal-phase silica gel. 1-(Benzyloxy carbonylamino)-3,6-dioxa-8-aminooctane and 2-(methylamino-methyl)phenylboronic acid **2** were synthesised according to literature procedures.[33,34]

NMR spectra were measured on Bruker DPX300, AV400, or AMX500 instruments and were assigned using COSY, HMBC, HMQC and DEPT spectra where appropriate. Coupling constants J are given in hertz (Hz); multiplicities are given as singlet (s), doublet (d), triplet (t), quartet (q), quintet (qn), sextet (sxt), septet (spt), or multiplet (m); broad signals are

indicated by (br). Due to quadrupolar relaxation, the aryl carbon atoms attached directly to boron are not always observed by ^{13}C NMR.[24] Electrospray mass spectra were measured on Micromass Prospec and Micromass Platform spectrometers; samples were prepared using 50 : 50 : 0.1 acetonitrile–water–formic acid solution. High resolution mass spectra (HRMS) were made on a Thermo Finnegan MAT95 XP instrument. Infrared spectra were recorded on a Bruker Alpha-P spectrometer and analysed using OPUS 6.5 software package. Elemental analysis was performed using a Thermo Scientific FLASH 2000 Series CHNS/O Analyzer. UV-Visible absorption measurements used Sigma Spectrophotometer Silica (Quartz) cuvettes (10 mm pathlength) and were recorded on a Jasco V660 spectrophotometer with Jasco EHC-716 Peltier temperature control. Fluorescence spectroscopy was carried out on a Perkin-Elmer LS55 fluorimeter, with an attached Julabo F25-HE water circulator for temperature control. All pH measurements were recorded on a HANNA pH 212 microprocessor pH meter using a Hamilton MINITRODE pH electrode that was calibrated using Fisher Chemicals standard buffer solutions (pH 4.0 – phthalate, 7.0 – phosphate, and 10.0 – borate). Unless otherwise stated all binding constants and pK_a values were determined at 20 °C.

Synthesis of compound 3

N-[8′-(**Benzyloxycarbonylamino**)-3′,6′-**dioxaaminooctyl**]-3α,7α,12α-**trihydroxy-5β-cholan-24-amide.** To a solution of cholic acid (1 g, 2.4 mmol) in dry dimethylformamide (20 mL) was added *O*-(benzotriazol-1-yl)-*N*,*N*,*N*′,*N*′-tetramethyluronium hexafluorophosphate (HBTU, 0.91 g, 2.4 mmol, 1 eq.) and *N*,*N*-diisopropylethylamine (DIPEA, 0.42 mL, 2.4 mmol, 1 eq.). The reaction mixture was stirred for 1 hour, over which time the solution took on a yellow coloration, indicating the formation of the active benzotriazolyl ester. A solution of 1-(benzyloxy-carbonylamino)-3,6-dioxa-8-aminooctane (0.68 g, 2.4 mmol, 1 eq.) in dry dimethylformamide (5 mL) was then added to the solution, which was stirred overnight. The solution was diluted with dichloromethane (50 mL) and washed successively with dilute hydrochloric acid (1 M, 25 mL), saturated sodium hydrogen carbonate solution (25 mL) and brine (25 mL). The organic layer was dried over magnesium sulphate, filtered, and the filtrate evaporated *in vacuo*. Flash chromatography (SiO_2, eluent: ethyl acetate–methanol 9 : 1 v/v) of the residue provided the title compound as a white foam (1.06 g, 66%). ^{1}H-NMR (400 MHz, CD_3OD, 25 °C): δ_H ppm 0.58 (3H, s, $C^{18/19}$ CH_3), 0.79 (3H, s, $C^{18/19}$ CH_3), 0.91 (3H, d, J = 4.7 Hz, $C^{21}H_3$), 1.15–2.22 (24H, steroid CH/CH_2), 3.33 (5H, t, J = 5.1 Hz, 2 × NCH_2 + C^3H), 3.43–3.53 (8H, m, $CH_2OCH_2CH_2OCH_2$), 3.73 (1H, m, C^7H), 3.86 (4H, m, $C^{12}H$ + OH), 5.02 (2H, s, $PhCH_2$), 5.68 (1H, br t, J = 5.2 Hz, amide NH), 6.65 (1H, br, carbamate NH), 7.27 (5H, m, CH_{Ar}). ^{13}C-NMR (100 MHz, CD_3OD, 25 °C): δ_C ppm 12.5, 17.4, 22.5, 23.3, 26.3, 27.6, 28.1, 30.4, 31.7, 33.1, 34.7, 34.8, 35.4, 35.5, 39.2, 39.4, 39.5, 40.8, 41.6, 46.4, 46.5, 66.7, 68.4, 69.9, 70.0, 70.1, 70.2, 71.8, 73.1, 128.1, 128.2, 128.5, 136.6, 156.7, 174.5. MS (ES+): *m/z* 673.5 [M + H]$^+$, 695.6 [M + Na]$^+$, 1346.3 [2M + H]$^+$.

2580 | *Org. Biomol. Chem.*, 2014, **12**, 2576–2583

This journal is © The Royal Society of Chemistry 2014

(8′-Amino-3′,6′-dioxaaminooctyl)-3α,7α,12α-trihydroxy-5β-cholan-24-amide. To a solution of N-[8′-(benzyloxycarbonyl-amino)-3′,6′-dioxaaminooctyl]-3α,7α,12α-trihydroxy-5β-cholan-24-amide (0.2 g, 0.3 mmol) in methanol (10 mL) was added acetic acid (1.7 µL, 0.03 mmol) and 10% palladium on activated charcoal (0.02 g). The reaction vessel was degassed three times and stirred under hydrogen overnight. The solution was filtered over Celite and evaporated in vacuo before the addition of dichloromethane (10 mL); the organic layer was washed successively with saturated sodium hydrogen carbonate solution (25 mL) and brine (25 mL). The organic layer was dried over magnesium sulphate, filtered, and the filtrate evaporated in vacuo to yield the title compound as a pale yellow oil (0.16 g, 99%). ^{1}H-NMR (400 MHz, CD$_3$OD, 25 °C): δ_H ppm 0.71 (3H, s, C$^{18/19}$ CH$_3$), 0.92 (3H, s, C$^{18/19}$ CH$_3$), 1.03 (3H, d, J = 6.5 Hz, C^{21}H$_3$), 1.28–2.34 (24H, steroid CH/CH$_2$), 3.15 (2H, t, J = 5.3 Hz, CH$_2$NH$_2$), 3.38 (2H, t, J = 4.7, NHCH$_2$) 3.58 (2H, t, J = 5.9, NHCH$_2$CH$_2$), 3.69 (4H, s, OCH$_2$CH$_2$O), 3.73 (2H, t, J = 5.1 Hz, CH$_2$CH$_2$NH$_2$), 3.82 (1H, m, C^{7}H), 3.97 (1H, m, C^{12}H). ^{13}C-NMR (100 MHz, CD$_3$OD, 25 °C): δ_C ppm 13.1, 17.9, 23.3, 24.4, 28.0, 28.8, 29.7, 31.0, 31.3, 33.4, 34.2, 36.0, 36.6, 37.1, 40.3, 40.6, 40.8, 41.1, 43.2, 43.3, 47.6, 48.1, 68.0, 69.2, 70.8, 71.4, 71.5, 73.0, 74.2, 177.2. MS (ES+): m/z 539.5 [M + H]$^+$. HRMS for C$_{30}$H$_{54}$N$_2$O$_6$: expected 539.4015, found 539.4017.

(8′-((2-Boronobenzyl)amino)-3′,6′-dioxaaminooctyl)-3α,7α,12α-trihydroxy-5β-cholan-24-amide (3). To a solution of (8′-amino-3′,6′-dioxaaminooctyl)-3α,7α,12α-trihydroxy-5β-cholan-24-amide (0.1 g, 0.19 mmol) in anhydrous methanol (5 mL) was added 2-formylphenylboronic acid (28 mg, 0.19 mmol) and stirred for 45 minutes. The reaction mixture was cooled to 0 °C and sodium borohydride (36 mg, 0.95 mmol) was added slowly portionwise, the resulting solution was stirred for 45 minutes at 0 °C and for a further 3 hours at room temperature. The solution was diluted with dichloromethane (20 mL) and washed successively with dilute HCl (1 M, 5 mL), saturated sodium hydrogen carbonate solution (5 mL) and brine (5 mL). The organic layer was dried over magnesium sulphate, filtered and the filtrate evaporated in vacuo to yield the title compound 3 as a white foam (116 mg, 91%). ^{1}H-NMR (400 MHz, CD$_3$OD, 25 °C): δ_H ppm 0.70 (3H, s, C$^{18/19}$ CH$_3$), 0.92 (3H, s, C$^{18/19}$ CH$_3$), 1.01 (3H, d, J = 6.7 Hz, C^{21}H$_3$), 1.05–2.35 (24 H steroid CH/CH$_2$), 3.09 (2H, t, J = 5.7 Hz, CH$_2$NH), 3.29 (2H, t, J = 5.7 Hz, NH$_{amide}$CH$_2$), 3.36 (1H, m, C^{3}H), 3.53 (2H, t, J = 5.1 Hz, NH$_{amide}$CH$_2$CH$_2$), 3.67 (4H, m, OCH$_2$CH$_2$O), 3.81 (3H, t, J = 5.4 Hz, CH$_2$CH$_2$NH + C^{7}H), 3.95 (1H, m, C^{12}H), 4.07 (2H, s, PhCH$_2$), 7.12–7.24 (3H, m, CH$_{Ar}$), 7.39–7.45 (1H, m, CH$_{Ar}$). ^{13}C-NMR (100 MHz, CD$_3$OD, 25 °C): δ_C ppm 13.1, 17.8, 23.2, 24.3, 27.9, 28.8, 29.6, 31.2, 33.3, 34.1, 35.9, 36.5, 37.0, 40.2, 40.5, 41.0, 43.0, 43.2, 48.1, 48.2, 49.1, 49.3, 54.9, 68.0, 69.0, 70.7, 71.2, 71.4, 72.9, 74.0, 79.5, 126.8, 127.7, 128.4, 128.9, 129.2, 131.5, 176.9. MS (ES$^+$): m/z 637.5 (100%) [M − 2H$_2$O + H]$^+$, 673.6 [M + H]$^+$. HRMS for C$_{37}$H$_{57}$BN$_2$O$_6$: expected 637.4388, found 637.4372. Elemental analysis for C$_{37}$H$_{62}$BN$_2$O$_9$·CH$_2$Cl$_2$: expected C: 58.92%, H: 8.33%, N: 3.62%; found C: 58.46%, H: 8.19%, N: 3.41%. ν_{max}/cm^{-1} 3357 (OH), 2930, 2869, 1649, 1214, 1076, 745.

Procedure for HPTS fluorescent assay of metal ion transport for boronocholates with and without fructose present

A lipid thin film was first prepared by the addition of spectroscopic grade chloroform to egg yolk phosphatidylcholine (EYPC, 40 mg, 52 µmol) and cholesterol (5 mg, 13 µmol) in a round bottomed flask (5 mL). Chloroform was slowly evaporated in vacuo at room temperature to leave a lipid thin film on the interior of the flask. HPTS phosphate buffer (1.2 mL, 100 µM HPTS, 20 mM M$_n$H$_m$PO$_4$, 100 mM MCl, pH 6.5 where M$^+$ = Na$^+$ or K$^+$ as appropriate) was added, followed by detachment of the lipid film from the interior of the flask by vortex agitation, and extruded through a polycarbonate membrane (200 nm pore size, 19×). To remove unencapsulated HPTS, an aliquot of the suspension (1 mL) was diluted with phosphate buffer (1.5 mL, pH 6.5) and purified by gel permeation chromatography (GPC) on a PD10 desalting column (eluted with 3.5 mL phosphate buffer). This provided a purified suspension of HPTS-encapsulated vesicles (15.5 mM total lipid concentration).

An aliquot (25 µL) of the vesicle suspension was transferred to a fluorescence cuvette containing phosphate buffer (1.975 mL, 20 mM M$_n$H$_n$PO$_4$, 100 mM MCl, pH 8.5 where M$^+$ = Na$^+$ or K$^+$ as appropriate) with stirring (0.19 mM total lipid concentration) and fluorescence measurements were immediately started (ex. 405 nm and 460 nm, em. 510 nm, time interval 8 s) as a function of time. After 180 s the relevant ionophore was added (20 µL, 0.01 mM total ionophore concentration, 5 mol%) and vesicles were lysed after 1200 s by the addition of Triton X-100 (25 µL, 25% v/v in distilled water). The change in the normalized ratio I_{460}/I_{405} as a function of time gave the rate of M$^+$/OH$^-$ antiport across the phospholipid bilayer. The above procedure was repeated at fructose concentrations of 0.25 mM, 0.5 mM, 10 mM, 0.1 M, 0.5 M, achieved by ensuring each buffer composition contained the relevant concentration of fructose.

U-tube metal picrate transport experiments

A chloroform solution of the potentially transporting species (1 mM, 5 mL) was transferred to a glass U-tube (internal diameter 10 mm) and incubated at 25 °C. To one side of the U-tube was added a receiving phase of phosphate buffer (2.5 mL, 20 mM Na$_n$H$_m$PO$_4$, 100 mM NaCl, pH 6.5), and to the other side was added a source phase of 0.01% sodium picrate in phosphate buffer (2.5 mL, 20 mM Na$_n$H$_m$PO$_4$, 100 mM NaCl, pH 8.5). Addition of the source phase marked the start of the experiment; aliquots (1 mL) were taken at intervals from the receiving phase and analysed for the presence of picrate by UV spectroscopy (356 nm); after each measurement the sample was immediately replaced back in the receiving phase of the U-tube. The chloroform was stirred (300 rpm) for the entire experiment to aid diffusion through to the receiving phase.

U-tube fructose transport experiments

A chloroform solution of the potentially transporting species (1 mM, 5 mL) was transferred to a glass U-tube (internal

diameter 10 mm) incubated at 25 °C. To one side of the U-tube was added a receiving phase of phosphate buffer (2.5 mL D$_2$O containing 0.75% % 3-(trimethylsilyl)propionic-2,2,3,3-d$_4$ acid as an internal standard, 20 mM Na$_n$H$_m$PO$_4$, 100 mM NaCl, pH 6.5), and to the other side was added a source phase of fructose (1 M) and 0.01% sodium picrate in phosphate buffer (2.5 mL D$_2$O containing 0.75% 3-(trimethylsilyl)propionic-2,2,3,3-d4 acid as an internal standard, 20 mM Na$_n$H$_m$PO$_4$, 100 mM NaCl, pH 8.5). Addition of the source phase marked the start of the experiment; aliquots (0.8 mL) were taken at intervals from the receiving phase and analysed for the presence of D-fructose by ^{1}H NMR spectroscopy, after each measurement the sample was immediately replaced back to the receiving phase of the U-tube. The chloroform was stirred (300 rpm) for the entire experiment to aid diffusion through to the receiving phase.

Distribution coefficient determinations

Solutions of relevant ionophores were prepared in 1-octanol (10 mM, 0.5 mL) and sodium phosphate buffer (20 mM Na$_n$H$_m$PO$_4$, 100 mM NaCl, pH 8.5) was added (0.5 mL). The aqueous–organic mixture was vigorously mixed using a vortex mixer for 180 s before standing for 1 h to allow separation of the organic and aqueous layers. Aliquots (100 µL) of the 1-octanol layer were transferred to a UV-visible cuvette containing HPLC-grade methanol (1.9 mL) and mixed before measurement (260 nm). The procedure was repeated for different fructose concentrations in sodium phosphate buffer (20 mM Na$_n$H$_m$PO$_4$, 100 mM NaCl, pH 8.5, [fructose] = 0.01, 0.1, 0.5 mol L^{-1}). To provide a maximum absorbance reading solutions of relevant ionophores were prepared in 1-octanol (5 mM, 100 µL) and transferred to a UV-visible cuvette containing HPLC-grade methanol (1.9 mL, 0.25 mM total ionophore concentration) and mixed before measurement (260 nm).

Binding constant estimation with (2-methylamino methylphenyl)boronic acid 2

Following the protocol of Wang et al.,[22] a three-component competitive assay with pyrocatechol violet[28] was used to determine the binding constant between **2** and fructose. Two experiments were conducted to determine the equilibrium constants of the competitive system. First, the association for **2** with pyrocatechol violet (PV) was determined (K_{eq1}). A solution of PV (2.74 mM, 2 mL) in phosphate buffer (20 mM Na$_n$H$_m$PO$_4$, 100 mM NaCl, pH 8.5) was transferred to a UV-visible cuvette and a solution of **2** in PV-phosphate buffer (2.74 mM PV, 20 mM Na$_n$H$_m$PO$_4$, 100 mM NaCl, pH 8.5) was titrated into the cuvette. A plot of changes in absorbance (596 nm) as a function of the concentration of **2**, and subsequent iterative non-linear curve fitting (Dynafit[35]) of the data provided the binding constant for the PV-**2** complex (K_{eq1}).

The binding constant for the **2**-fructose complex (K_{eq2}) was found by titrating a PV-**2** solution with fructose. The binding

constant K_{eq2} was determined by plotting $1/P$ as a function of Q, where P is defined as:

$$P = [L_o] - \frac{1}{QK_{eq1}} - \frac{[I_o]}{Q+1} \quad (3)$$

where L_o is the total amount of boronic acid, I_o is the total amount of PV, K_{eq1} is the binding constant of the PV-**2** complex, and Q is the ratio of the concentration of free PV to complexed PV,

$$A = \frac{[I]}{[IL]} \quad (4)$$

where I is the concentration of free PV in solution, and IL is the concentration of complexed PV in solution. The binding constant for **2** with a diol can be calculated by dividing K_{eq1} by the gradient of a plot of $1/P$ vs. Q.

References

1 (a) R. Nishiyabu, Y. Kubo, T. D. James and J. S. Fossey, *Chem. Commun.*, 2011, **47**, 1106–1123; (b) S. D. Bull, M. G. Davidson, J. M. H. Van Den Elsen, J. S. Fossey, A. T. A. Jenkins, Y.-B. Jiang, Y. Kubo, F. Marken, K. Sakurai, J. Zhao and T. D. James, *Acc. Chem. Res.*, 2013, **46**, 312–326; (c) R. A. Brown, V. Diemer, S. J. Webb and J. Clayden, *Nat. Chem.*, 2013, **5**, 853–860.

2 (a) H. Kim, Y. J. Kang, S. Kang and K. T. Kim, *J. Am. Chem. Soc.*, 2012, **134**, 4030–4033; (b) G. A. Ellis, M. J. Palte and R. T. Raines, *J. Am. Chem. Soc.*, 2012, **134**, 3631–3634; (c) Y. Li, W. Xiao, K. Xiao, L. Berti, J. Luo, H. P. Tseng, G. Fung and K. S. Lam, *Angew. Chem., Int. Ed.*, 2012, **51**, 2864–2869.

3 (a) C. Lu, H. Li, H. Wang and Z. Liu, *Anal. Chem.*, 2013, **85**, 2361–2369; (b) Y. Liu, L. Ren and Z. Liu, *Chem. Commun.*, 2011, **47**, 5067–5069.

4 (a) L. He, D. E. Fullenkamp, J. G. Rivera and P. B. Messersmith, *Chem. Commun.*, 2011, **47**, 7497–7499; (b) Y. Kotsuchibashi, R. V. C. Agustin, J.-Y. Lu, D. G. Hall and R. Narain, *ACS Macro Lett.*, 2013, **2**, 260–264.

5 (a) O. Savsunenko, H. Matondo, S. Franceschi-Messant, E. Perez, A. F. Popov, I. Rico-Lattes, A. Lattes and Y. Karpichev, *Langmuir*, 2013, **29**, 3207–3213; (b) A. Kashiwada, M. Tsuboi, N. Takamura, E. Brandenburg, K. Matsuda and B. Koksch, *Chem.–Eur. J.*, 2011, **17**, 6179–6186; (c) A. Kashiwada, M. Tsuboi, T. Mizuno, T. Nagasaki and K. Matsuda, *Soft Matter*, 2009, **5**, 4719–4725; (d) E. Han, L. Ding and H. Ju, *Anal. Chem.*,

2582 | *Org. Biomol. Chem.*, 2014, **12**, 2576–2583

This journal is © The Royal Society of Chemistry 2014

2011, **83**, 7006–7012; (*e*) A. Mahalingam, A. R. Geonnotti, J. Balzarini and P. F. Kiser, *Mol. Pharm.*, 2011, **8**, 2465–2475.

6 (*a*) M. Berube, M. Dowlut and D. G. Hall, *J. Org. Chem.*, 2008, **73**, 6471–6479; (*b*) M. Dowlut and D. G. Hall, *J. Am. Chem. Soc.*, 2006, **128**, 4226–4227.

7 P. J. Duggan, T. A. Houston, M. J. Kiefel, S. M. Levonis, B. D. Smith and M. L. Szydzik, *Tetrahedron*, 2008, **64**, 7122–7126.

8 (*a*) T. Shinbo, K. Nishimura, T. Yamaguchi and M. Sugiura, *J. Chem. Soc., Chem. Commun.*, 1986, 349–351; (*b*) M.-F. Paugam, L. S. Valencia, B. Boggess and B. D. Smith, *J. Am. Chem. Soc.*, 1994, **116**, 11203–11204; (*c*) L. K. Mohler and A. W. Czarnik, *J. Am. Chem. Soc.*, 1993, **115**, 7037–7038.

9 (*a*) P. R. Westmark and B. D. Smith, *J. Pharm. Sci.*, 1996, **85**, 266–269; (*b*) P. R. Westmark, S. J. Gardiner and B. D. Smith, *J. Am. Chem. Soc.*, 1996, **118**, 11093–11100.

10 (*a*) M.-F. Paugam, G. T. Morin and B. D. Smith, *Tetrahedron Lett.*, 1993, **34**, 7841–7844; (*b*) G. T. Morin, M. P. Hughes, M.-F. Paugam and B. D. Smith, *J. Am. Chem. Soc.*, 1994, **116**, 8895–8901; (*c*) G. T. Morin, M.-F. Paugam, M. P. Hughes and B. D. Smith, *J. Org. Chem.*, 1994, **59**, 2724–2128.

11 J. T. Bien, M. Shang and B. D. Smith, *J. Org. Chem.*, 1995, **60**, 2147–2152.

12 J. C. Norrild and H. Eggert, *J. Chem. Soc., Perkin Trans. 2*, 1996, 2583–2588.

13 S. Hagihara, H. Tanaka and S. Matile, *J. Am. Chem. Soc.*, 2008, **130**, 5656–5657.

14 S. Litvinchuk, N. Sordé and S. Matile, *J. Am. Chem. Soc.*, 2005, **127**, 9316–9317.

15 (*a*) C. P. Wilson and S. J. Webb, *Chem. Commun.*, 2008, 4007–4009; (*b*) C. P. Wilson, C. Boglio, L. Ma, S. L. Cockroft and S. J. Webb, *Chem.–Eur. J.*, 2011, **17**, 3465–3473.

16 (*a*) P. Bandyopadhyay, V. Janout, L. Zhang, J. A. Sawko and S. L. Regen, *J. Am. Chem. Soc.*, 2000, **122**, 12888–12889; (*b*) P. Bandyopadhyay, V. Janout, L. Zhang and S. L. Regen, *J. Am. Chem. Soc.*, 2001, **123**, 7691–7696; (*c*) M. Mehiri, W.-H. Chen, V. Janout and S. L. Regen, *J. Am. Chem. Soc.*, 2009, **131**, 1338–1339; (*d*) L. Ma, M. Melegari, M. Colombini and J. T. Davis, *J. Am. Chem. Soc.*, 2008, **130**, 2938–2939; (*e*) Y. Zhao, H. Cho, L. Widanapathirana and S. Zhang, *Acc. Chem. Res.*, 2013, **46**, 2763–2772.

17 M. Yoshii, M. Yamamura, A. Satake and Y. Kobuke, *Org. Biomol. Chem.*, 2004, **2**, 2619–2623.

18 S. J. Gardiner, B. D. Smith, P. J. Duggan, M. J. Karpa and G. J. Griffin, *Tetrahedron*, 1999, **55**, 2857–2864.

19 S. Matile, N. Sakai and A. Hennig, *Transport Experiments in Membranes published in Supramolecular Chemistry: From Molecules to Nanomaterials*, John Wiley & Sons, Ltd., 2012.

20 J. Yan, H. Fang and B. Wang, *Med. Res. Rev.*, 2005, **25**, 490–520.

21 (*a*) J. Yan, G. Springsteen, S. Deeter and B. Wang, *Tetrahedron*, 2004, **60**, 11205–11209; (*b*) M. Vanduin, J. A. Peters, A. P. G. Kieboom and H. Vanbekkum, *Tetrahedron*, 1984, **40**, 2901–2911; (*c*) P. A. Sienkiewicz and D. C. Roberts, *J. Inorg. Nucl. Chem.*, 1980, **42**, 1559–1575.

22 G. Springsteen and B. H. Wang, *Tetrahedron*, 2002, **58**, 5291–5300.

23 D. J. Cabral, J. A. Hamilton and D. M. Small, *J. Lipid Res.*, 1986, **27**, 334–343.

24 C. J. Ward, P. Patel and T. D. James, *J. Chem. Soc., Perkin Trans. 1*, 2002, 462–470.

25 A. Adamczyk-Woźniak, K. M. Borys, I. D. Madura, A. Pawełko, E. Tomecka and K. Żukowski, *New J. Chem.*, 2013, **37**, 188–194.

26 Both compounds exhibited a significant lag period due to slow diffusion though the chloroform phase under our experimental conditions. See A. Giannetto, S. Lanza, F. Puntoriero, M. Cordaroa and S. Campagna, *Chem. Commun.*, 2013, **49**, 7611–7613.

27 M. J. Karpa, P. J. Duggan, G. J. Griffin and S. J. Freudigmann, *Tetrahedron*, 1997, **53**, 3669–3678.

28 Z. Zhong and E. V. Anslyn, *J. Am. Chem. Soc.*, 2002, **124**, 9014–9015.

29 (*a*) V. Gorteau, G. Bollot, J. Mareda and S. Matile, *Org. Biomol. Chem.*, 2007, **5**, 3000–3012; (*b*) B. D. Smith, J. P. Davis, S. P. Draffin and P. J. Duggan, *Supramol. Chem.*, 2004, **16**, 87–90.

30 J.-P. Behr, M. Kirch and J.-M. Lehn, *J. Am. Chem. Soc.*, 1985, **107**, 241–246.

31 J. R. D. Brown, PhD thesis, University of Manchester, 2013.

32 T. A. Houston, *ChemBioChem*, 2010, **11**, 954–957.

33 B. C. Roy and S. Mallik, *J. Org. Chem.*, 1999, **64**, 2969–2974.

34 K. M. K. Swamy, Y. J. Jang, M. S. Park, H. S. Koh, S. K. Lee, Y. J. Yoon and J. Yoon, *Tetrahedron Lett.*, 2005, **46**, 3453–3456.

35 P. Kuzmic, *Anal. Biochem.*, 1996, **237**, 260–273.

This journal is © The Royal Society of Chemistry 2014

Org. Biomol. Chem., 2014, **12**, 2576–2583 | **2583**